
Learning Neuro-Symbolic Relational Transition Models for Bilevel Planning

Rohan Chitnis*, Tom Silver*,
Joshua B. Tenenbaum, Tomás Lozano-Pérez, Leslie Pack Kaelbling
 MIT Computer Science and Artificial Intelligence Laboratory
 {ronuchit, tslvr, jbt, tlp, lpk}@mit.edu

Abstract

Despite recent, independent progress in model-based reinforcement learning and integrated symbolic-geometric robotic planning, synthesizing these techniques remains challenging because of their disparate assumptions and strengths. In this work, we take a step toward bridging this gap with Neuro-Symbolic Relational Transition Models (NSRTs), a novel class of transition models that are data-efficient to learn, compatible with powerful robotic planning methods, and generalizable over objects. NSRTs have both symbolic and neural components, enabling a bilevel planning scheme where symbolic AI planning in an outer loop guides continuous planning with neural models in an inner loop. Experiments in four robotic planning domains show that NSRTs can be learned after only tens or hundreds of training episodes, and then used for fast planning in new tasks that require up to 60 actions to reach the goal and involve many more objects than were seen during training. Video: <https://tinyurl.com/chitnis-nsrts>

1 Introduction

For robots to function effectively in the world, they will need to be able to plan across a wide range of spatial and temporal scales, and also to learn flexibly and quickly to solve problems for which they were not specifically designed. Robotic planning and model-based reinforcement learning (MBRL) methods have each made great progress in recent years, tackling different aspects of this challenge. Synthesizing them, however, has proven challenging because of their disparate assumptions and strengths. Robotic task and motion planning (TAMP) combines symbolic AI planning with geometric motion planning to solve long-horizon, goal-based planning tasks with continuous state and action spaces [Garrett et al., 2021, Srivastava et al., 2014, Kaelbling and Lozano-Pérez, 2011]. TAMP systems are typically learning-free, relying on hand-specified symbolic models and low-level geometric primitives to plan. MBRL methods [Moerland et al., 2020] generally make fewer assumptions, requiring the agent to learn a transition model of its environment from data. Their limited inductive bias, though, makes them unable to scale to the kinds of tasks that TAMP can solve.

How can we design a system that learns transition models, as in MBRL, for planning in TAMP tasks? To cope with continuous spaces and long horizons, a common approach is for the agent to first plan in an *abstraction*, and then *refine* that plan into actions it can execute [Nilsson, 1984, Konidaris et al., 2018, Lyu et al., 2019, Ahmetoglu et al., 2020]. There has been recent interest in planning with *symbolic* abstractions compatible with AI planners [Yang et al., 2018, Lyu et al., 2019, Gordon et al., 2019]. However, such approaches make a critical *downward refinability* assumption, which posits that a valid symbolic plan can always be refined into a sequence of actions that solves the task [Bacchus and Yang, 1994]. A major motivation for TAMP is that downward refinability is *not* a reasonable assumption in robotics, because geometric constraints are hard to express with symbolic abstractions.

*Equal contribution

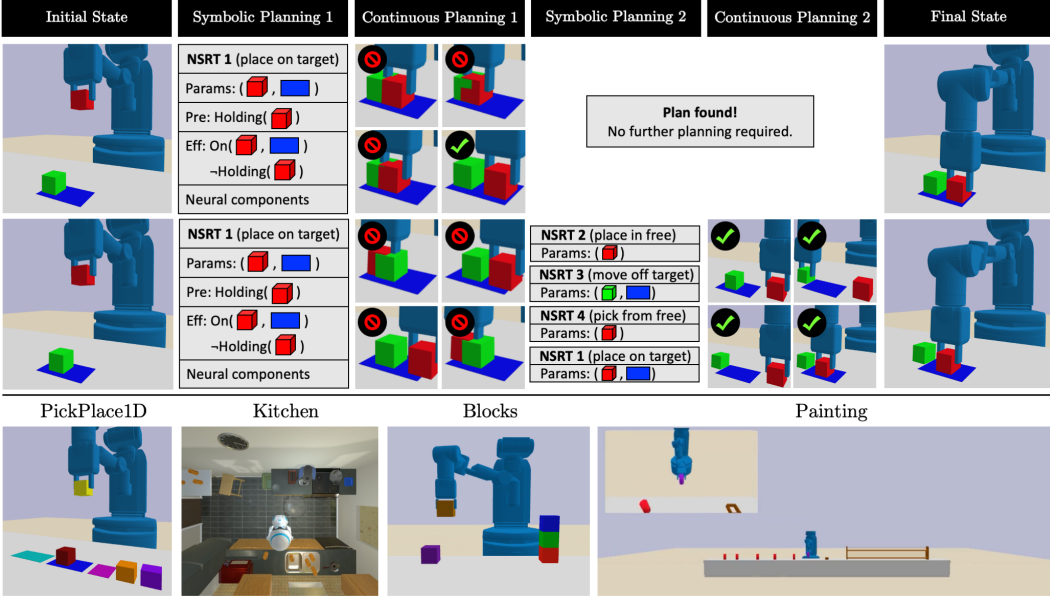


Figure 1: We propose Neuro-Symbolic Relational Transition Models (NSRTs) for integrated symbolic and geometric reasoning. (Top row) Given the goal of moving the red block onto the blue target, we first perform AI planning with the symbolic components of the NSRTs to find a one-step symbolic plan. The Continuous Planning 1 column shows various ways in which the agent attempts to *refine* this one-step symbolic plan into a ground action, using the neural components of NSRT 1; it finds a collision-free refinement, shown in the Final State column. (Middle row) Here, the green block is initially in a slightly different position, such that the red block has no room to be placed onto the blue target. The initial symbolic plan is the same. However, this symbolic plan is not *downward refinable*, so Continuous Planning 1 fails. The agent then continues on to consider a four-step symbolic plan that first moves the green object away (Symbolic Planning 2 column), which is successfully refined in the Continuous Planning 2 column. This example illustrates that in the presence of complex geometric constraints which make symbolic abstractions lossy, integrated symbolic and geometric reasoning is necessary. (Bottom row) Screenshots of our four robotic planning environments. Kitchen uses the AI2-THOR simulator [Kolve et al., 2017]; the others use PyBullet [Coumans and Bai, 2016].

In this paper, we propose a novel transition model class for learning and planning in multi-task, long-horizon, goal-based settings with continuous state and action spaces, such as those illustrated in Figure 1 (bottom row). Our planning strategy draws on TAMP, performing integrated symbolic and geometric planning to avoid the downward refinability assumption. Following previous work, we assume that a small number of *predicates* (named relations over objects) are given, having been implemented by a human engineer [Chitnis et al., 2016, Lyu et al., 2019, Gordon et al., 2019, Illanes et al., 2020, Silver et al., 2021, Wang et al., 2021], or learned from previous experience in similar domains. Importantly, because downward refinability does not hold, we must view these predicates as *lossy abstractions* of the continuous state space. See Figure 1 (top and middle rows) for an example.

Our main contribution is the **Neuro-Symbolic Relational Transition Model** (NSRT) (pronounced “insert”), a transition model class that can be efficiently learned and used for planning at scale. NSRTs have both (1) symbolic components, which use the given predicates to define an abstract transition model, and (2) neural components, which sample actions and predict transitions in the environment. This two-level structure affords bilevel neuro-symbolic planning, with symbolic AI planning in an outer loop serving as guidance for continuous planning with neural models in an inner loop. All components are relational, permitting generalization to problems with new and more objects.

This paper focuses on *how to learn NSRTs* and *how to use NSRTs for planning* in continuous-space, long-horizon tasks. We show in four robotic planning domains, across both the PyBullet [Coumans and Bai, 2016] and AI2-THOR [Kolve et al., 2017] simulators, that NSRTs can be learned in only tens or hundreds of training episodes. We also show in these domains that NSRTs allow for fast planning

on test tasks, with many more objects than during training and long horizons of up to 60 actions. Baseline comparisons confirm that integrated neuro-symbolic reasoning is key to these successes.

2 Related Work

Model-Based Reinforcement Learning. Our work addresses transition model learning in relational settings, and is closely related to the field of relational MBRL. Many recent approaches to deep MBRL learn unstructured neural transition models, and therefore must resort to highly undirected planning strategies like the cross-entropy method [Hamrick et al., 2021, Hafner et al., 2020, 2021, Nagabandi et al., 2018, Chua et al., 2018, Pertsch et al., 2020b]. Some recent MBRL work has used more powerful planners, such as RRTs [Ichter et al., 2020], LQR [Chebotar et al., 2017], divide-and-conquer MCTS [Parascandolo et al., 2020], and policy search with GPs [Deisenroth and Rasmussen, 2011]. Relational MBRL is a subfield of MBRL that uses relational learning [Džeroski et al., 2001, Tadepalli et al., 2004] to learn object-centric factored transition models [Battaglia et al., 2016, Chang et al., 2017, Kansky et al., 2017] or to discover STRIPS operator models [Xia et al., 2019, Lang et al., 2012] when given a set of predicates. Our work also learns relational transition models, but the main distinction is that our models are compatible with integrated symbolic and geometric planners.

Symbolic AI Planning for RL. Our work continues a recent line of investigation that seeks to leverage symbolic AI planners in learning settings with continuous states and actions. For example, previous work has considered learning propositional [Zhang et al., 2018, Dittadi et al., 2020, Konidaris et al., 2018, Tsividis, 2019] or lifted [Arora et al., 2018, Chitnis et al., 2021, Asai and Fukunaga, 2018, Asai, 2019, Asai and Muise, 2020, Ames et al., 2018, Ahmetoglu et al., 2020] symbolic transition models, and using them with AI planners [Hoffmann, 2001, Helmert, 2006]. Other related work has used symbolic planners as managers in hierarchical RL, where low-level option policies are learned [Lyu et al., 2019, Sarathy et al., 2020, Gordon et al., 2019, Illanes et al., 2020, Yang et al., 2018, Kokel et al., 2021]. In contrast to all these, we are focused on robotic settings where the planner must handle *geometric* considerations in addition to the symbolic ones.

Learning for Robotic Task and Motion Planning. Integrated symbolic and geometric planning is key to task and motion planning (TAMP); see Garrett et al. [2021] for a survey. While TAMP systems can plan effectively at long horizons [Kaelbling and Lozano-Pérez, 2011, Srivastava et al., 2014, Garrett et al., 2018], they typically require hand-specified symbolic models and action samplers, and a known low-level transition model. Recent work has addressed learning the symbolic model [Loula et al., 2020, Silver et al., 2021], the action samplers [Wang et al., 2021, Chitnis et al., 2016, Kim et al., 2018], and even abstract heuristics [Kim and Shimanuki, 2019, Driess et al., 2020]. In contrast, our approach jointly learns the symbolic model, action samplers, and transition model.

3 Problem Setting

We study transition model learning in multi-task settings, where tasks are deterministic and goal-based, with continuous actions and object-oriented continuous states. Formally, we consider an *environment* $\langle \mathcal{T}, d, \mathcal{A}, f, \mathcal{P} \rangle$ and a collection of *tasks*, each of which is a tuple $\langle s_0, g, H \rangle$.

Environments. \mathcal{T} is a set of object types, and $d : \mathcal{T} \rightarrow \mathbb{Z}^+$ defines the dimensionality of the real-valued attribute (feature) vector of each object type. For example, an object of type “box” might have an attribute vector describing its current pose, side length, and color. A state s is a mapping from a set of typed objects o to attribute vectors of dimension $d(o)$, where $d(o)$ is shorthand for the dimension of the attribute vector of the type of object o . We use \mathcal{S} to denote the state space. $\mathcal{A} \subseteq \mathbb{R}^m$ is the continuous action space. $f : \mathcal{S} \times \mathcal{A} \rightarrow \mathcal{S} \cup \mathcal{C}$ is a deterministic transition function that maps a state s and action a to either a next state in \mathcal{S} , or a collision $c \in \mathcal{C}$, which is represented as a set of objects that collided with each other or the agent, when a was taken from s . A collision set c is only outputted if it is non-empty, i.e. $c \neq \emptyset$. *Throughout this work, the transition function f is unknown. The agent only observes states and collisions through online interaction with the environment.*

\mathcal{P} is a set of *predicates* given to the agent. A predicate is a named, binary-valued relation among some number of objects. A *ground atom* applies a predicate to specific objects, such as $\text{ABOVE}(o_1, o_2)$, where the predicate is ABOVE . A *lifted atom* applies a predicate to typed placeholder variables: $\text{ABOVE}(\mathbf{?}a, \mathbf{?}b)$. For our purposes, all predicates are discrete; their arguments are objects, not continuous values. Taken together, the set of ground atoms that hold in a continuous state define

a *discrete state abstraction*; let $\text{PARSE}(s)$ denote the abstract state for state $s \in \mathcal{S}$. For instance, a state s where objects o_1 , o_2 , and o_3 are stacked may be represented by the abstract state $\text{PARSE}(s) = \{\text{ON}(o_1, o_2), \text{ON}(o_2, o_3)\}$. Note that this abstract state loses details about the geometry of the scene.

Tasks and Objective. A task $\langle s_0, g, H \rangle$ is an initial state $s_0 \in \mathcal{S}$, a goal g , and a planning horizon H . We will generally denote the set of objects in s_0 as \mathcal{O} , which is fixed within a task (but *not* between tasks). Goals g are sets of ground atoms over the object set \mathcal{O} , such as $\{\text{ON}(o_3, o_2), \text{ON}(o_2, o_1)\}$. The agent interacts with the environment *episodically*. An episode begins with the initial state s_0 of a task. The agent then takes actions sequentially, observing the current state and any collisions at each timestep. If the agent encounters a state s for which $g \subseteq \text{PARSE}(s)$, the episode is *solved*. An episode finishes when it is solved, when any collision is encountered, or after H timesteps. Tasks are split into training tasks and test tasks; generally, the test tasks will have more objects and longer horizons. The test tasks are not known to the agent before evaluation. The agent’s objective is to maximize the number of episodes solved with tasks drawn from the set of test tasks.

Data Collection. In this work, we are focused on the problems of *learning* and *planning*. To isolate these, we use a simple, fixed strategy for exploration that makes use of a *behavior prior* $\pi_0(\cdot | s)$, a state-conditioned distribution over \mathcal{A} . Recent work has studied learning behavior priors [Pertsch et al., 2020a, Singh et al., 2021, Ajay et al., 2021]; we are assuming it is given, but it could be learned. In comparison to, e.g., reward shaping or demonstrations, one advantage of the behavior prior is that it will allow for targeted ablation studies (methods B6 and B7 in Section 7). Data-gathering proceeds by running π_0 episodically on tasks sampled from the set of training tasks. We do not use π_0 at test time. Note that this strategy assumes that exploration with π_0 is safe, either because the environment is inherently safe (e.g., a simulator) or because π_0 has safety guarantees. Since the exploration policy is fixed and given, our setting can be seen as *offline reinforcement learning* [Levine et al., 2020].

4 Neuro-Symbolic Relational Transition Models (NSRTs)

The next three sections introduce Neuro-Symbolic Relational Transition Models (NSRTs). In this section, we describe the NSRT representation; in Section 5, we address planning with NSRTs; and in Section 6, we discuss learning NSRTs. Figure 2 will be a useful reference throughout these sections.

We want models that are *learnable*, *plannable*, and *generalizable*. How can we leverage the structure in our setting — object-oriented states and discrete predicates — to achieve these? First, following previous work, we seek representations that are relational, leading to data-efficient learning and generalization over objects [Battaglia et al., 2018]. The difference is our focus on settings where integrated symbolic and continuous reasoning are necessary. We thus arrive at the following definition:

A **Neuro-Symbolic Relational Transition Model** (NSRT) is a tuple $\langle O, P, E, \pi, h \rangle$, where:

- $O = (o_1, \dots, o_k)$ are ordered *parameters*; each o_i is a placeholder for an object of some type.
- P is a set of *symbolic preconditions*; each precondition is a lifted atom over O .
- E is a set of *symbolic effects*; each effect is a (possibly negated) lifted atom over O .
- $\pi(a | v_s)$ is an *action sampler*, a conditional distribution over actions $a \in \mathcal{A}$, where $v_s \in \mathbb{R}^{d(o_1) + \dots + d(o_k)}$ is a vector of concatenated object attribute values.
- $h : \mathbb{R}^{d(o_1) + \dots + d(o_k)} \times \mathcal{A} \rightarrow \mathbb{R}^{d(o_1) + \dots + d(o_k)}$ is a *low-level effect model*, which predicts next object attribute values given current object attribute values and an action.

A *ground NSRT* is an NSRT with each parameter $o_i \in O$ mapped to an object from \mathcal{O} in the task.

The **symbolic components** O , P , and E are designed to facilitate search through the discrete abstract state space defined by the predicates. Note that all these components involve only objects, types, and predicates; the continuous object attribute values and the continuous actions do not play a role. These components also define operators in symbolic AI planning [Bonet and Geffner, 2001, Hoffmann, 2001, Helmert, 2006]; we use this connection to our advantage in planning (Section 5).

What is the relationship between the symbolic components of an NSRT and the continuous environment? We adopt the following *weak semantics*: given a task with object set \mathcal{O} , for any ground NSRT over \mathcal{O} with ground preconditions \bar{P} and ground effects \bar{E} , *there exists* some state $s \in \mathcal{S}$, and some action $a \in \mathcal{A}$, such that $\bar{P} \subseteq \text{PARSE}(s)$ and $\bar{E} = (\text{PARSE}(s') - \text{PARSE}(s)) \cup \neg(\text{PARSE}(s) - \text{PARSE}(s'))$, where $s' = f(s, a)$ did not yield collisions. These semantics do *not* assume downward refinability, which would have required the above “*there exists* some state” to be “*for all* states.”

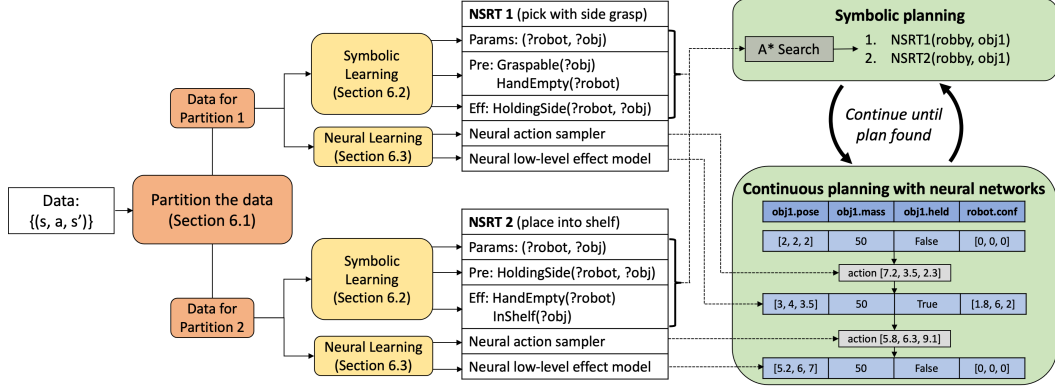


Figure 2: Diagram of our overall pipeline, with a simplified example from the Painting environment. An NSRT (Section 4) contains symbolic components (parameters, preconditions, and effects) used for A^* search with AI planning heuristics, and neural components (action sampler, low-level effect model) used for continuous planning. Here, the robot must be side-grasping an object in order to place it into a shelf, as illustrated by the NSRTs in the middle. We can learn both the symbolic and the neural components of NSRTs from transition data (Section 6), and then perform bilevel planning with the learned NSRTs (Section 5). Negative effects are omitted from this figure for visual clarity.

The **neural components** π and h help implement the inner loop of bilevel planning, which searches over actions $a \in \mathcal{A}$ using guidance from the abstract search (we will describe this further in Section 5). The action sampler π takes as input the concatenated attribute values of all NSRT parameters, and outputs actions. The fact that π is stochastic can be important for planning, where multiple sampling tries may be required to achieve the desired effects (e.g., see Figure 1, or see Section 4.1 of Wang et al. [2021]). The low-level effect model h takes the same input as the action sampler, along with an action; it predicts new concatenated attribute values resulting from executing that action. This h can be seen as a transition model where the states of all objects *not* in the parameters are predicted to not change. We emphasize that neither π nor h is tied to any specific objects: when an NSRT is grounded with objects, the inputs to π and h are grounded to the attribute values of those objects in a state. This relational structure leads to data-efficient training and generalization over objects.

What is the relationship between the neural and symbolic components? First, the low-level effect model h need only predict transitions for states where the preconditions P hold. Second, the action sampler π is responsible for sampling only actions that achieve the effects E . For instance, suppose a ground NSRT has the effect $IN SHELF(o_1)$; then, π should only select actions that would put o_1 in the shelf. This targeted, effect-specific sampling proves very important for efficient planning. These relationships imply π and h are “locally scoped,” responsible for only a subset of transition space.

5 Bilevel Neuro-Symbolic Planning with NSRTs

We now describe how the structure of NSRTs can be exploited for bilevel planning. Recall that our weak semantics of NSRT symbolic preconditions and effects (Section 4) do *not* guarantee downward refinability. Therefore, finding a valid abstract state sequence does *not* necessarily mean that we can find actions to refine the sequence. So, we will perform bilevel planning with an outer search in the abstract space informing an inner search over continuous actions; to account for the lack of downward refinability, we will continue the outer search when the inner one is unable to find a solution.

Let a *symbolic plan* be a sequence of ground NSRTs, and a *plan* be a sequence of actions $a \in \mathcal{A}$. A symbolic plan achieves the goal g (at the symbolic level) starting from initial state s_0 if, upon applying all NSRT effects successively starting from $\text{PARSE}(s_0)$, we have that (1) all NSRT preconditions are satisfied and (2) g is a subset of the resulting final abstract state. A plan, by contrast, achieves g starting at s_0 if successive application of the unknown transition model f , starting from s_0 and taking the actions in the plan, results in no collisions and a final state s_{final} where $g \subseteq \text{PARSE}(s_{\text{final}})$.

Symbolic Planning. Our outer search will produce candidate symbolic plans that the inner search will attempt to *refine* into plans using the neural components of each NSRT in the symbolic plan. This

particular planning strategy falls under the broad class of search-then-sample TAMP techniques [Garrett et al., 2021]. Concretely, our outer search runs A^* from $\text{PARSE}(s_0)$ to g . The heuristic we use, h_{add} , is a domain-independent heuristic drawn from the symbolic planning literature [Bonet and Geffner, 2001] that approximates the distance from a state to the goal under a *delete relaxation* of the symbolic model, constructed by ignoring negative effects. This A^* search will efficiently find candidate symbolic plans that achieve the goal according to the NSRT preconditions and effects.

Continuous Planning. For each candidate symbolic plan, the inner search attempts to refine it into a plan using the neural components of the NSRTs. We use the action sampler π in conjunction with the low-level effect model h of each NSRT in the symbolic plan to construct an *imagined* state-action trajectory starting from the initial state s_0 . Planning is successful if the goal g holds in the final imagined state of this trajectory. For efficiency, as we compute each state s in this imagined trajectory, we check whether $\text{PARSE}(s)$ equals the expected abstract state according to the high-level A^* search. If not, we have deviated from the abstract state sequence defined by this symbolic plan, and so we terminate and return control to the A^* search, which continues on to find a new candidate symbolic plan. We can now understand why it is so crucial that the action sampler for each NSRT is specific to *that NSRT*’s symbolic effects; this property is what allows us to either produce actions that follow the desired abstract state sequence, or give up refining if any π is unable to produce such an action.

Handling Collisions. Recall that in our problem setting, an episode ends when a collision occurs. Following Srivastava et al. [2014], we would like to use the occurrence of a collision during continuous planning to inform symbolic planning. In Appendix A.1, we describe a simple domain-independent procedure for learning to predict collisions and using this learned model during continuous planning. This optimization propagates collision information back to the symbolic level and guides search away from plans that would repeat the situations in which collisions were previously predicted.

6 Learning NSRTs

We now address learning the symbolic (Section 6.2) and neural (Section 6.3) components of NSRTs.

6.1 Partitioning the Transition Data

Recall that data collection (Section 3) gathers a set of samples from the unknown transition model f : each sample is a state $s \in \mathcal{S}$, an action $a \in \mathcal{A}$, and either a next state $s' \in \mathcal{S}$ or collision set $c \in \mathcal{C}$. We will ignore the transitions that led to collisions here; they will be used in Appendix A.1. Thus, we have a dataset of transitions $\tau = (s, a, s')$. We begin by partitioning this transition data in such a way that each partition will ultimately correspond to a single NSRT, thus automatically determining the number of learned NSRTs. Our partitioning algorithm uses four subroutines that operate over transitions. The first is **EFFECTS**, which maps a transition $\tau = (s, a, s')$ to the symbolic effects $(\text{PARSE}(s') - \text{PARSE}(s)) \cup \neg(\text{PARSE}(s) - \text{PARSE}(s'))$. The second is **REF**, which maps a transition τ to a subset of the objects in the state. Intuitively, these are the objects that were “involved” in the transition[†]. In practice, we implement **REF**(τ) by selecting all objects that either appear in **EFFECTS**(τ) or exhibit some change in continuous state. This implementation suffices for our experiments, but it cannot capture “action at a distance,” where some object influences a transition without itself changing; more conservative implementations of **REF** could be used instead, perhaps at some cost to planning and learning efficiency. The third subroutine is **PROJECT**, which takes in a transition τ and uses **REF** to create a “projected transition” $\underline{\tau} = (\underline{s}, a, \underline{s'})$, where only the attribute values for objects in **REF**(τ) are included in \underline{s} and $\underline{s'}$. The fourth subroutine is **UNIFY**, which takes two projected transitions $\underline{\tau}_1, \underline{\tau}_2$ and searches for a mapping from objects in $\underline{\tau}_1$ to objects in $\underline{\tau}_2$ such that **EFFECTS**($\underline{\tau}_1$) and **EFFECTS**($\underline{\tau}_2$) are equivalent under the mapping, and such that there is a correspondence between the object attributes that changed in the transitions. If such a mapping exists, we say that the two projected transitions *can be unified*. With these four subroutines, we can partition the data: two transitions τ_1 and τ_2 are in the same partition if and only if the projected transitions **PROJECT**(τ_1) and **PROJECT**(τ_2) can be unified. We will now learn one NSRT per partition.

[†]This subroutine is related to *deictic references* [Pasula et al., 2007, Xia et al., 2019], with the difference being that deictic references are functions of state and action alone, rather than state, action, and next state.

6.2 Learning the Symbolic Components

We now show how to learn NSRT parameters O , symbolic preconditions P , and symbolic effects E for a single partition. Let τ^* be an arbitrary transition from the partition; we can generate the parameters O by creating placeholder objects of the same types as the objects in $\text{REF}(\tau^*)$. Then, for every transition τ in the partition, we use UNIFY to construct object-to-parameter mappings $\sigma_\tau : \text{REF}(\tau) \rightarrow O$. Note that σ_τ is a bijection; let σ_τ^{-1} be its inverse. For symbolic preconditions and effects, we use a simple inductive approach from the literature on learning AI planning operators [Bonet et al., 2019]; it restricts learning by assuming that for each lifted effect set seen in the data, there is exactly one lifted precondition set. After partitioning, the symbolic effects for all transitions within a single partition are equivalent up to object remapping. Thus, we create symbolic effects $E = \sigma_{\tau^*}[\text{EFFECTS}(\underline{\tau^*})]$, where $\sigma_{\tau^*}[\cdot]$ denotes substitution of all objects with the NSRT parameters. Then, we create symbolic preconditions by intersecting all lifted abstract states in the partition: $P = \bigcap_{\tau=(s,\cdot,\cdot)} \sigma_\tau[\text{PARSE}(\underline{s})]$.

6.3 Learning the Neural Components

We now describe how to learn low-level effect models h and action samplers π for each partition’s NSRT. The key idea is to use the state projections computed during partitioning to create regression problems. Let $s[o]$ be the attribute vector for object o in state s , and the NSRT parameters be $O = (o_1, o_2, \dots, o_k)$. Given a transition $\tau = (s, a, s')$ in this partition with projection $\underline{\tau} = (\underline{s}, a, \underline{s}')$, we can convert \underline{s} into a 1D vector $v_s = \underline{s}[\sigma_\tau^{-1}(o_1)] \circ \dots \circ \underline{s}[\sigma_\tau^{-1}(o_k)]$, where \circ denotes concatenation. In words, v_s is a vector of the attribute values in state s corresponding *only* to the objects that map the ground atoms $\text{EFFECTS}(\tau)$ to the lifted atoms E of the NSRT. We can do the same to produce $v_{s'}$ for \underline{s}' . Applying this procedure to all transitions in the partition gives us a dataset $(v_s, a, v_{s'})$.

The problem of learning h now reduces to regression, with v_s and a being the inputs and $v_{s'}$ being the output. We use a standard fully connected neural network (NN) to implement the regression model, and train it to minimize the mean-squared error over the data. Furthermore, in our robotic environments of interest, transitions are often *sparse*, changing only a subset of object attributes at any given time. We exploit this observation by calculating the attributes that change in *any* transition within a partition, and only predict next values for those attributes, leaving the others unchanged.

Learning π requires *distribution* regression, where we must fit $P(a | v_s)$ to the transitions (v_s, a, \cdot) . We use a fully connected NN that takes v_s as input and predicts the mean μ and covariance matrix Σ of a Gaussian distribution. This NN is trained to maximize the likelihood of action a under $\mathcal{N}(\mu, \Sigma)$, averaged over the data. We restrict Σ to be diagonal and positive semi-definite using an exponential linear unit [Clevert et al., 2016]. Since Gaussians have limited expressivity (e.g., they are unimodal), we also learn an *applicability classifier* that maps pairs (v_s, a) to 0 or 1. This classifier should check that s satisfies the NSRT preconditions and that taking a satisfies the NSRT effects. We implement this as a fully connected NN with binary cross-entropy loss. To create negative examples, we use data from other partitions, or data from the same partition but with the objects re-mapped. Altogether, to sample from π , we rejection sample from the Gaussian until the applicability classifier outputs a 1.

7 Experiments

Our empirical evaluations address the following key questions: **(Q1)** Can NSRTs be learned data-efficiently? **(Q2)** Can learned NSRTs be used to plan to long horizons, especially in tasks involving new and more objects than were seen during training? **(Q3)** Is bilevel planning efficient and effective, and are both levels needed? **(Q4)** To what extent are learned action samplers useful for planning?

7.1 Experimental Setup

We evaluate the four key questions above by running eight methods across four environments. All experiments were run on Ubuntu 18.04 using 4 CPU cores of an Intel Xeon Platinum 8260 processor.

Environments. In this section, we describe our four environments at a high level, with details in Appendix A.2. The environments are illustrated in Figure 1 (bottom row). Each has three sets of tasks: training, “easy” test, and “hard” test. “Hard” test tasks require generalization to more objects.

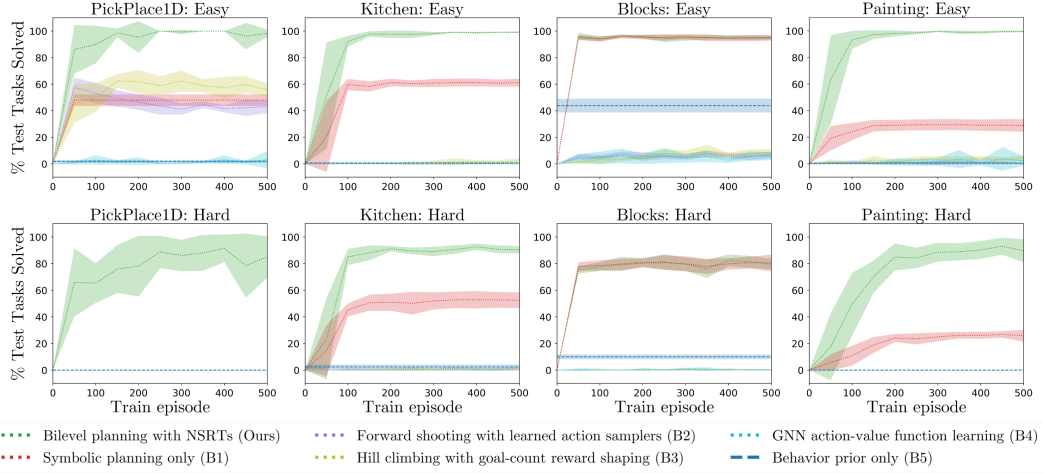


Figure 3: Learning curves for every environment, showing the percentage of 100 randomly generated test tasks (top row: easy tasks; bottom row: hard tasks) solved as a function of the number of training episodes. Each curve depicts a mean over 8 seeds, with standard deviation shaded. All methods are given a timeout of 3 seconds per task. We can see that our method (green) quickly learns to solve many more tasks than all the baselines, especially in the hard tasks of each environment.

- *Environment 1:* In “PickPlace1D,” a robot must pick blocks and place them into designated target regions on a table. All pick and place poses are 1D. Some placements are obstructed by movable objects; none of the predicates capture obstructions, leading to a lack of downward refinability.
- *Environment 2:* In “Kitchen,” a robot waiter must pick cups, fill them with water, wine, or coffee, and serve them to customers. Some cups are too heavy to be lifted; the cup masses are not represented by the predicates, leading to a lack of downward refinability.
- *Environment 3:* In “Blocks,” modeled after classic AI blocksworld, a robot must stack blocks on a table to make towers. In this environment only, the downward refinability assumption holds.
- *Environment 4:* In “Painting,” a robot must pick, wash, dry, paint, and place widgets into a box or shelf. Placing into the box (shelf) requires picking with a top (side) grasp. All widgets must be painted a particular color before being placed, which first requires washing/drying if the widget starts off dirty or wet. The box has a lid that may obstruct placements; whether the lid will obstruct a placement is not represented symbolically, leading to a lack of downward refinability.

Methods Evaluated. We evaluate the following methods. See Appendix A.3 for additional details.

- *Ours: Bilevel planning with NSRTs.* This is our main approach. Plans are executed open-loop.
- *B1: Symbolic planning only.* This baseline performs symbolic planning using the symbolic components of the learned NSRTs. When a symbolic plan is found that reaches the goal, it is immediately executed by calling the learned action samplers for the corresponding ground NSRTs in sequence, open-loop. The learned low-level effect models are not used. This baseline ablates away the integrated nature of our planner, instead assuming that downward refinability holds (i.e., once a valid symbolic plan is found, no further symbolic planning would ever need to be done).
- *B2: Forward shooting with learned action samplers.* This baseline randomly samples H -length sequences of ground NSRTs and uses their neural components to imagine a trajectory, repeating until it finds a trajectory where the final state satisfies the goal. This baseline does not use the symbolic components of the NSRTs, and thus can be seen as an ablation of the symbolic planning.
- *B3: Hill climbing with goal-count reward shaping.* This baseline performs local search over full plans. At each iteration, a random plan step is resampled using the learned action sampler of a random NSRT. The new plan is rejected unless it improves the number of goal atoms satisfied in the final imagined state. As in B2, the symbolic components of the NSRTs are not used.
- *B4: GNN action-value function learning.* This “model-free” baseline trains a goal-conditioned graph neural network (GNN) action-value function using fitted Q-iteration. The GNN takes as input a continuous low-level state, the corresponding abstract state, and a continuous action; it outputs expected discounted future returns. At evaluation time, given a state, we draw several candidate actions from the behavior prior π_0 , and take the action with the highest predicted value.

Methods	PickPlace1D		Kitchen		Blocks		Painting	
	Easy	Hard	Easy	Hard	Easy	Hard	Easy	Hard
Bilevel planning with NSRTs (Ours)	98.4	85.0	99.1	90.4	95.0	79.6	99.6	89.6
Bilevel planning with prior (B6)	95.9	46.4	71.9	32.6	89.9	53.4	84.5	0.1
Forward shooting with prior (B7)	71.1	0.0	0.0	1.5	62.9	8.6	5.4	0.0

Table 1: Percentage of 100 randomly generated test tasks solved after 500 episodes of training. Each number is a mean over 8 seeds; bold results are within one standard deviation of best (Appendix A.4).

- *B5: Behavior prior only.* This baseline takes actions that are directly sampled from the prior π_0 .
- *B6: Bilevel planning with prior.* This method is an ablation of our main method that does not use the learned NSRT action samplers π . Instead, actions are selected by rejection sampling from the prior π_0 , with rejections determined by checking the learned applicability classifier (Section 6.3).
- *B7: Forward shooting with prior.* This baseline uses the forward shooting strategy of B2 with rejection sampling from π_0 , like B6. Only the low-level effect models h of the NSRTs are used.

All methods except B5 (which does not do any learning) receive the exact same data.

7.2 Results and Discussion

We provide learning curves comparing our method with B1-B5 in Figure 3. The main observation is that in all environments, our method quickly learns to solve tasks within the allotted 3-second timeout. Thus, key questions **Q1** and **Q2** can be answered affirmatively. Turning next to **Q3**, we can study whether bilevel planning is effective by comparing Ours, B1, and B2. The gap between Ours and B1 in most environments shows the importance of integrated bilevel planning, where the low-level planning with neural networks is tightly coupled with the abstract, symbolic search. B1 will not be effective in any environment where downward refinability does not hold — only Blocks is downward refinable, which explains why Ours and B1 perform identically on it. B2, meanwhile, fails to solve even a single task in most environments, indicating that leveraging the symbolic components of NSRTs for providing planning guidance is extremely important. Since B2 learns the same NSRTs as Ours (the data is the same), the large gap in performance is due solely to planning, not learning.

Both B3 and B4 are generally ineffective. B3 performs local search, which is much weaker than our directed A*. B4 is model-free, forgoing planning in favor of learning an action-value function directly; such strategies are known to be more data-hungry [Moerland et al., 2020]. B5 does not require any training, and is just included to illustrate how far one can get by simply executing actions sampled from the behavior prior. B5 performs decently in some environments, but the gap between Ours and B5 suggests that we are learning something meaningful instead of just imitating the prior.

To evaluate **Q4**, we turn to an ablation study. Table 1 compares our method with B6 and B7, both of which rejection sample from the generic behavior prior π_0 rather than using our learned NSRT action samplers. First, comparing B6 and B7, bilevel planning is much better than shooting, which speaks to the benefits of using the symbolic components of the NSRTs to guide the continuous-space planning; this conclusion was also supported by our main plot in Figure 3. Second, comparing Ours and B6, the learned action samplers help substantially versus rejection sampling from the behavior prior. This is because the behavior prior is highly generic, not targeted toward any specific set of effects like the learned action samplers are, meaning rejection sampling will often take many tries.

8 Conclusion, Limitations, and Future Work

We proposed NSRTs, a new class of transition models that are well-suited for long-horizon, goal-based, object-oriented planning tasks. We showed that their neuro-symbolic structure affords fast bilevel planning, and found experimentally that they are data-efficient to learn and generalize effectively.

Key limitations of the current work include: (1) that we are assuming predicates are given; (2) that a behavior prior is given which guides data collection; (3) that transitions are sparse, involving only a fixed number of objects (the NSRT parameters); (4) that environments are deterministic and fully observable. To address (1), we would like to combine NSRTs with recent work on learning predicates from high-dimensional inputs [Konidaris et al., 2018, Asai and Fukunaga, 2018, Asai, 2019, Asai and Muise, 2020]. Next, (2) can be addressed by drawing on recent advances in skill

prior learning for RL [Pertsch et al., 2020a, Singh et al., 2021, Ajay et al., 2021] to pre-train this prior, either from demonstrations or from a curriculum of simple “atomic” tasks like grasping and placing. We addressed a special case of (3) by learning a separate model that uses the full state to anticipate collisions; future work could generalize this idea beyond collisions. For (4), we hope to draw on recent techniques in TAMP for dealing with stochasticity [Garrett et al., 2020] and partial observability [Hadfield-Menell et al., 2015, Kaelbling and Lozano-Pérez, 2013]. A necessary change here would be to allow NSRTs to predict distributions over both symbolic and low-level effects.

References

A. Ahmetoglu, M. Y. Seker, A. Sayin, S. Bugur, J. Piater, E. Oztop, and E. Ugur. Deepsym: Deep symbol generation and rule learning from unsupervised continuous robot interaction for planning. *arXiv preprint arXiv:2012.02532*, 2020.

A. Ajay, A. Kumar, P. Agrawal, S. Levine, and O. Nachum. OPAL: Offline primitive discovery for accelerating offline reinforcement learning. In *International Conference on Learning Representations*, 2021.

Y. Alkhazraji, M. Frorath, M. Grützner, M. Helmert, T. Liebetraut, R. Mattmüller, M. Ortlieb, J. Seipp, T. Springenberg, P. Stahl, and J. Wülfing. Pyperplan, 2020. URL <https://doi.org/10.5281/zenodo.3700819>.

B. Ames, A. Thackston, and G. Konidaris. Learning symbolic representations for planning with parameterized skills. In *2018 IEEE/RSJ International Conference on Intelligent Robots and Systems (IROS)*, pages 526–533. IEEE, 2018.

A. Arora, H. Fiorino, D. Pellier, M. Etivier, and S. Pesty. A review of learning planning action models. *Knowledge Engineering Review*, 33, 2018.

M. Asai. Unsupervised grounding of plannable first-order logic representation from images. In *Proceedings of the International Conference on Automated Planning and Scheduling*, volume 29, pages 583–591, 2019.

M. Asai and A. Fukunaga. Classical planning in deep latent space: Bridging the subsymbolic-symbolic boundary. In *Proceedings of the AAAI Conference on Artificial Intelligence*, volume 32, 2018.

M. Asai and C. Muise. Learning neural-symbolic descriptive planning models via cube-space priors: The voyage home (to STRIPS). In *Proceedings of the Twenty-Ninth International Joint Conference on Artificial Intelligence, IJCAI-20*, pages 2676–2682, 2020.

F. Bacchus and Q. Yang. Downward refinement and the efficiency of hierarchical problem solving. *Artificial Intelligence*, 71(1):43–100, 1994.

P. W. Battaglia, R. Pascanu, M. Lai, D. J. Rezende, and K. Kavukcuoglu. Interaction networks for learning about objects, relations and physics. In *Advances in Neural Information Processing Systems*, 2016.

P. W. Battaglia, J. B. Hamrick, V. Bapst, A. Sanchez-Gonzalez, V. Zambaldi, M. Malinowski, A. Tacchetti, D. Raposo, A. Santoro, R. Faulkner, et al. Relational inductive biases, deep learning, and graph networks. *arXiv preprint arXiv:1806.01261*, 2018.

B. Bonet and H. Geffner. Planning as heuristic search. *Artificial Intelligence*, 129(1-2):5–33, 2001.

B. Bonet, G. Frances, and H. Geffner. Learning features and abstract actions for computing generalized plans. In *Proceedings of the AAAI Conference on Artificial Intelligence*, volume 33, pages 2703–2710, 2019.

M. B. Chang, T. Ullman, A. Torralba, and J. B. Tenenbaum. A compositional object-based approach to learning physical dynamics. In *International Conference on Learning Representations*, 2017.

Y. Chebotar, K. Hausman, M. Zhang, G. Sukhatme, S. Schaal, and S. Levine. Combining model-based and model-free updates for trajectory-centric reinforcement learning. In *Proceedings of the 34th International Conference on Machine Learning*, volume 70, pages 703–711, 2017.

R. Chitnis, D. Hadfield-Menell, A. Gupta, S. Srivastava, E. Groshev, C. Lin, and P. Abbeel. Guided search for task and motion plans using learned heuristics. In *Robotics and Automation (ICRA), 2016 IEEE International Conference on*, pages 447–454. IEEE, 2016.

R. Chitnis, T. Silver, J. Tenenbaum, L. P. Kaelbling, and T. Lozano-Pérez. GLIB: Efficient exploration for relational model-based reinforcement learning via goal-literal babbling. In *Proceedings of the AAAI Conference on Artificial Intelligence*, 2021.

K. Chua, R. Calandra, R. McAllister, and S. Levine. Deep reinforcement learning in a handful of trials using probabilistic dynamics models. In *Advances in Neural Information Processing Systems*, volume 31, 2018.

D. Clevert, T. Unterthiner, and S. Hochreiter. Fast and accurate deep network learning by exponential linear units (elus). In *4th International Conference on Learning Representations*, 2016.

E. Coumans and Y. Bai. PyBullet, a python module for physics simulation for games, robotics and machine learning. *GitHub repository*, 2016.

M. Deisenroth and C. E. Rasmussen. PILCO: A model-based and data-efficient approach to policy search. In *Proceedings of the 28th International Conference on machine learning (ICML-11)*, pages 465–472, 2011.

A. Dittadi, F. K. Drachmann, and T. Bolander. Planning from pixels in atari with learned symbolic representations. *arXiv preprint arXiv:2012.09126*, 2020.

D. Driess, J.-S. Ha, and M. Toussaint. Deep visual reasoning: Learning to predict action sequences for task and motion planning from an initial scene image. In *Proc. of Robotics: Science and Systems (R:SS)*, 2020.

S. Džeroski, L. De Raedt, and K. Driessens. Relational reinforcement learning. *Machine learning*, 43(1):7–52, 2001.

C. R. Garrett, T. Lozano-Pérez, and L. P. Kaelbling. Stripstream: Integrating symbolic planners and blackbox samplers. *arXiv preprint arXiv:1802.08705*, 2018.

C. R. Garrett, C. Paxton, T. Lozano-Pérez, L. P. Kaelbling, and D. Fox. Online replanning in belief space for partially observable task and motion problems. In *2020 IEEE International Conference on Robotics and Automation (ICRA)*, pages 5678–5684. IEEE, 2020.

C. R. Garrett, R. Chitnis, R. Holladay, B. Kim, T. Silver, L. P. Kaelbling, and T. Lozano-Pérez. Integrated task and motion planning. *Annual review of control, robotics, and autonomous systems*, 4:265–293, 2021.

D. Gordon, D. Fox, and A. Farhadi. What should I do now? Marrying reinforcement learning and symbolic planning. *arXiv preprint arXiv:1901.01492*, 2019.

D. Hadfield-Menell, E. Groshev, R. Chitnis, and P. Abbeel. Modular task and motion planning in belief space. In *2015 IEEE/RSJ International Conference on Intelligent Robots and Systems (IROS)*, pages 4991–4998. IEEE, 2015.

D. Hafner, T. Lillicrap, J. Ba, and M. Norouzi. Dream to control: Learning behaviors by latent imagination. In *International Conference on Learning Representations*, 2020.

D. Hafner, T. P. Lillicrap, M. Norouzi, and J. Ba. Mastering atari with discrete world models. In *International Conference on Learning Representations*, 2021.

J. B. Hamrick, A. L. Friesen, F. Behbahani, A. Guez, F. Viola, S. Witherspoon, T. Anthony, L. H. Buesing, P. Veličković, and T. Weber. On the role of planning in model-based deep reinforcement learning. In *International Conference on Learning Representations*, 2021.

M. Helmert. The fast downward planning system. *Journal of Artificial Intelligence Research*, 26: 191–246, 2006.

J. Hoffmann. FF: The fast-forward planning system. *AI magazine*, 22(3):57–57, 2001.

B. Ichter, P. Sermanet, and C. Lynch. Broadly-exploring, local-policy trees for long-horizon task planning. *arXiv preprint arXiv:2010.06491*, 2020.

L. Illanes, X. Yan, R. T. Icarte, and S. A. McIlraith. Symbolic plans as high-level instructions for reinforcement learning. In *Proceedings of the International Conference on Automated Planning and Scheduling*, volume 30, pages 540–550, 2020.

L. P. Kaelbling and T. Lozano-Pérez. Hierarchical task and motion planning in the now. In *Robotics and Automation (ICRA), 2011 IEEE International Conference on*, pages 1470–1477. IEEE, 2011.

L. P. Kaelbling and T. Lozano-Pérez. Integrated task and motion planning in belief space. *The International Journal of Robotics Research*, 32(9-10):1194–1227, 2013.

K. Kansky, T. Silver, D. A. Mély, M. Eldawy, M. Lázaro-Gredilla, X. Lou, N. Dorfman, S. Sidor, S. Phoenix, and D. George. Schema networks: Zero-shot transfer with a generative causal model of intuitive physics. In *International Conference on Machine Learning*, pages 1809–1818, 2017.

B. Kim and L. Shimanuki. Learning value functions with relational state representations for guiding task-and-motion planning. *Conference on Robot Learning*, 2019.

B. Kim, L. P. Kaelbling, and T. Lozano-Pérez. Guiding search in continuous state-action spaces by learning an action sampler from off-target search experience. In *Thirty-Second AAAI Conference on Artificial Intelligence*, 2018.

D. P. Kingma and J. Ba. Adam: A method for stochastic optimization. *arXiv preprint arXiv:1412.6980*, 2014.

H. Kokel, A. Manoharan, S. Natarajan, R. Balaraman, and P. Tadepalli. RePReLU: Integrating relational planning and reinforcement learning for effective abstraction. In *Thirty First International Conference on Automated Planning and Scheduling (ICAPS)*, 2021.

E. Kolve, R. Mottaghi, W. Han, E. VanderBilt, L. Weihs, A. Herrasti, D. Gordon, Y. Zhu, A. Gupta, and A. Farhadi. Ai2-thor: An interactive 3d environment for visual ai. *arXiv preprint arXiv:1712.05474*, 2017.

G. Konidaris, L. P. Kaelbling, and T. Lozano-Perez. From skills to symbols: Learning symbolic representations for abstract high-level planning. *Journal of Artificial Intelligence Research*, 61: 215–289, 2018.

T. Lang, M. Toussaint, and K. Kersting. Exploration in relational domains for model-based reinforcement learning. *The Journal of Machine Learning Research*, 13(1):3725–3768, 2012.

S. Levine, A. Kumar, G. Tucker, and J. Fu. Offline reinforcement learning: Tutorial, review, and perspectives on open problems. *arXiv preprint arXiv:2005.01643*, 2020.

J. Loula, K. Allen, T. Silver, and J. Tenenbaum. Learning constraint-based planning models from demonstrations. In *2020 IEEE/RSJ International Conference on Intelligent Robots and Systems (IROS)*, 2020.

D. Lyu, F. Yang, B. Liu, and S. Gustafson. SDRL: interpretable and data-efficient deep reinforcement learning leveraging symbolic planning. In *Proceedings of the AAAI Conference on Artificial Intelligence*, volume 33, pages 2970–2977, 2019.

T. M. Moerland, J. Broekens, and C. M. Jonker. Model-based reinforcement learning: A survey. *arXiv preprint arXiv:2006.16712*, 2020.

A. Nagabandi, G. Kahn, R. S. Fearing, and S. Levine. Neural network dynamics for model-based deep reinforcement learning with model-free fine-tuning. In *2018 IEEE International Conference on Robotics and Automation (ICRA)*, pages 7559–7566. IEEE, 2018.

N. J. Nilsson. Shakey the robot. Technical Report 323, AI Center, SRI International, 333 Ravenswood Ave., Menlo Park, CA 94025, Apr 1984.

G. Parascandolo, L. Buesing, J. Merel, L. Hasenclever, J. Aslanides, J. B. Hamrick, N. Heess, A. Neitz, and T. Weber. Divide-and-conquer monte carlo tree search for goal-directed planning. *arXiv preprint arXiv:2004.11410*, 2020.

H. M. Pasula, L. S. Zettlemoyer, and L. P. Kaelbling. Learning symbolic models of stochastic domains. *Journal of Artificial Intelligence Research*, 29:309–352, 2007.

K. Pertsch, Y. Lee, and J. J. Lim. Accelerating reinforcement learning with learned skill priors. *arXiv preprint arXiv:2010.11944*, 2020a.

K. Pertsch, O. Rybkin, F. Ebert, S. Zhou, D. Jayaraman, C. Finn, and S. Levine. Long-horizon visual planning with goal-conditioned hierarchical predictors. *Advances in Neural Information Processing Systems*, 33, 2020b.

O. Rivlin, T. Hazan, and E. Karpas. Generalized planning with deep reinforcement learning. *arXiv preprint arXiv:2005.02305*, 2020.

V. Sarathy, D. Kasenberg, S. Goel, J. Sinapov, and M. Scheutz. Spotter: Extending symbolic planning operators through targeted reinforcement learning. *arXiv preprint arXiv:2012.13037*, 2020.

T. Silver, R. Chitnis, J. Tenenbaum, L. P. Kaelbling, and T. Lozano-Perez. Learning symbolic operators for task and motion planning. *arXiv preprint arXiv:2103.00589*, 2021.

A. Singh, H. Liu, G. Zhou, A. Yu, N. Rhinehart, and S. Levine. Parrot: Data-driven behavioral priors for reinforcement learning. In *International Conference on Learning Representations*, 2021.

S. Srivastava, E. Fang, L. Riano, R. Chitnis, S. Russell, and P. Abbeel. Combined task and motion planning through an extensible planner-independent interface layer. In *Robotics and Automation (ICRA), 2014 IEEE International Conference on*, pages 639–646. IEEE, 2014.

P. Tadepalli, R. Givan, and K. Driessens. Relational reinforcement learning: An overview. In *Proceedings of the ICML-2004 workshop on relational reinforcement learning*, pages 1–9, 2004.

P. A. Tsividis. *Theory-based learning in humans and machines*. PhD thesis, Massachusetts Institute of Technology, 2019.

Z. Wang, C. R. Garrett, L. P. Kaelbling, and T. Lozano-Pérez. Learning compositional models of robot skills for task and motion planning. *The International Journal of Robotics Research*, 40(6-7): 866–894, 2021.

V. Xia, Z. Wang, K. Allen, T. Silver, and L. P. Kaelbling. Learning sparse relational transition models. In *International Conference on Learning Representations*, 2019.

F. Yang, D. Lyu, B. Liu, and S. Gustafson. PEORL: Integrating symbolic planning and hierarchical reinforcement learning for robust decision-making. In *International Joint Conference on Artificial Intelligence*, 2018.

A. Zhang, S. Sukhbaatar, A. Lerer, A. Szlam, and R. Fergus. Composable planning with attributes. In *International Conference on Machine Learning*, pages 5842–5851, 2018.

A Appendix

A.1 Handling Collisions in Learning and Planning

Handling Collisions in Planning. Here we describe how a collision prediction model can be used to optimize the planning method outlined in Section 5. In the paragraph below, we describe how to learn this model. The reason that this planning procedure is external to the rest of planning with NSRTs is that it uniquely involves propagating information from continuous planning back to symbolic planning. The procedure is a simplified domain-independent version of the domain-dependent error propagation method used in the popular TAMP system of Srivastava et al. [2014]. First, we introduce special predicates `NOTOBSTRUCTS` for every object type in the environment, and for each NSRT, we add a symbolic effect $\text{NOTOBSTRUCTS}(o_i)$ for each o_i in the parameters O . This says that every action affecting a set of objects clears all those objects from being obstructions; we found this simple technique to be sufficient for our experimental domains, but other, more domain-specific information can be leveraged instead. Finally, during refinement of a symbolic plan, if a non-empty collision set $\{o_1, \dots, o_j\}$ is predicted at any timestep, we immediately terminate the inner search, update the preconditions of the ground NSRT at that timestep to include $\{\text{NOTOBSTRUCTS}(o_1), \dots, \text{NOTOBSTRUCTS}(o_j)\}$, and restart the A* search from the initial state. Effectively, this change forces the planner to either consider actions which change the states of predicted obstructions before using the same ground NSRT, or just avoid using this ground NSRT entirely.

Learning to Predict Collisions. Here we address the problem of learning to anticipate collisions during planning. Note that unlike NSRT learning (Section 6), which is “locally scoped” to a fixed number of objects defined by the NSRT parameters, collision prediction can require reasoning about all objects in the full state. Recall that we have collision data of the form (s, a, c) , where $c \in \mathcal{C}$ is the set of objects in collision. We take a straightforward approach that suffices for our experimental domains: we train a graph neural network that takes as input s , $\text{PARSE}(s)$, and a , and outputs a score between 0 and 1 for each object, representing the predicted probability that it is included in the collision set $c = f(s, a)$. Graph neural networks are well-suited to this type of reasoning, because they are relational and can reason about continuous-valued dependencies. We create one node in the graph for each object in the task; the feature vector of each node includes the object’s attribute values and arity-1 ground atoms in $\text{PARSE}(s)$. Edges between nodes correspond to arity-2 ground atoms in $\text{PARSE}(s)$; higher-arity predicates can be converted into arity-2 ones [Rivlin et al., 2020]. For the output graph, each node has a single feature corresponding to the score. Once trained, we use this model to predict the collision set by including all objects whose score is over 0.5.

A.2 Extended Environment Details

Environment 1: In “PickPlace1D,” a robot must pick blocks and place them into designated target regions on a table. All pick and place poses lie along a 1D axis. There are three **object types**: blocks, targets, and obstructors. (The robot is abstracted away for simplicity.) Blocks have one **attribute**: a 1D pose. Targets have two: a start pose and an end pose. Obstructors have three: a start pose and an end pose, along with a third attribute indicating orthogonal distance from the 1D axis. **Actions** are 2D, with the first dimension representing a pose at which to execute a pick, and the second dimension representing a pose at which to place. Each action updates the state of at most one block or obstructor according to whether the pick pose is within a small tolerance of the object’s pose. Placing a block within some tolerance of an obstructor results in a collision. Picking and placing an obstructor always moves the obstructor away from the 1D axis, preventing future collisions. The **behavior prior** randomly chooses to pick obstructors or pick blocks that are not yet at their target region, and then place them away (for obstructors) or on a random target region (for blocks). There are three **predicates**: `ON(?BLOCK, ?TARGET)`, `INFREESPACE(?BLOCK)`, and `ISREMOVED(?OBSTRUCTION)`, with the semantics suggested by the names. Across all tasks, blocks start in free space, obstructors are each initially obstructing some target region, and goals are to move each block to be `ON` a unique target. **Training tasks** feature 2 or 5 blocks, 5 or 10 targets, and 0 or 1 obstructors, and have horizon $H = 10$. **Easy test tasks** feature 2 blocks, 5 targets, and 0 or 1 obstructors, and have horizon $H = 25$. **Hard test tasks** feature 4 blocks, 12 targets, and 2 obstructors, and have horizon $H = 25$.

Environment 2: In “Kitchen,” a robot waiter must pick cups, fill them with water, wine, or coffee, and serve them to customers. There are three **object types**: cups, customers, and robots. Cup **attributes** include 6D pose, mass, what liquid is in the cup (an integer indicating empty, water, wine, or coffee), whether the cup has been served (true or false), and whether or not the cup is currently held by a robot (true or false). Customer attributes include an integer ID and current drink. The singular robot attribute is a 1D gripper joint state. **Actions** are 5D: the first three dimensions represent the *xyz* pose of a cup to be picked, the fourth dimension represents the ID of a customer to be served, and the fifth represents a liquid to be poured. Given an action, if the *xyz* pose is close enough to an unserved cup, and that cup is not too heavy, the cup is picked; otherwise, if the customer ID matches that of some customer and a cup is currently held, the held cup is delivered to the corresponding customer; otherwise, if the liquid is close enough to water, wine, or coffee, and if a cup is held, then the respective liquid is poured into the cup. If the robot tries to pick up a cup that is too heavy, no change occurs in the environment. The **behavior prior** randomly picks cups, pours liquids, or serves cups to unserved customers. The **predicates** are: CUSTOMERHASCOFFEE(?CUSTOMER), CUSTOMERHASWATER(?CUSTOMER), CUSTOMERHASWINE(?CUSTOMER), GRIPPEROPEN(?ROBOT), HOLDING(?CUP), CUPUNSERVED(?CUP), CUPHASCOFFEE(?CUP), CUPHASWATER(?CUP), CUPHASWINE(?CUP). Across all tasks, there is only one robot; customers are initially unserved and cups are initially empty; and goals involve the CUSTOMERHASCOFFEE, CUSTOMERHASWATER, and CUSTOMERHASWINE predicates. **Training tasks** feature 2 or 3 cups and 1 customer, and have horizon $H = 10$. **Easy test tasks** feature 2 cups and 1 customer, and have horizon $H = 3$. **Hard test tasks** feature 3 cups and 2 customers, and have horizon $H = 6$.

Environment 3: In “Blocks,” modeled after the classic AI blocksworld domain, a robot must stack blocks on a table to make towers. There are two **object types**: blocks and robots. Block **attributes** include a 3D pose, whether or not the block is held (true or false), and whether or not the block has another block above it (true or false). Robot attributes include a 1D gripper joint state. **Actions** are 4D, with the dimensions representing target end effector *xyz* pose and target gripper joint state. When an action is taken, if the target end effector pose is close enough to a block, that block is clear from above, the target gripper state is open enough, and no other block is held, then the block is picked. If a block is already held, and the target end effector pose is close enough to a clear location on the table, then the block is placed on the table at that location; if, instead, the target end effector pose is close enough to a clear block, then the held block is stacked on top of the clear block. The **behavior prior** randomly picks a block, or attempts to place a block on the table or another block. The **predicates** are: ON(?BLOCK1, ?BLOCK2), ONTABLE(?BLOCK), GRIPPEROPEN(?ROBOT), HOLDING(?BLOCK), CLEAR(?BLOCK). Across all tasks, there is only one robot, and goals involve the ON predicate. **Training tasks** feature 3 or 4 blocks, and have horizon $H = 20$. **Easy test tasks** feature 3 blocks, and have horizon $H = 25$. **Hard test tasks** feature 5 or 6 blocks, and have horizon $H = 35$.

Environment 4: In “Painting,” a robot must pick, wash, dry, paint, and place widgets into a box or shelf. Placing into the box requires picking with a top grasp; placing into the shelf requires picking with a side grasp. The box has a lid that may obstruct placements; whether the lid will obstruct a placement is not represented symbolically. This environment was introduced by Silver et al. [2021]. There are five **object types**: widgets, boxes, lids, shelves, and robots. Widget **attributes** include 3D pose, 1D color, 1D wetness, 1D dirtiness, and whether or not the widget is held (true or false). Box and shelf attributes include only a 1D color. Lid attributes are 1D, indicating the degree to which the lid is open. Robot attributes include a 1D end effector rotation (modulating between top and side grasps) and a 1D gripper joint state. **Actions** are 8D: the first four dimensions are target end effector pose and rotation, the fifth dimension is target gripper joint state, the sixth dimension is a “water level,” the seventh dimension is a “heat level,” and the final dimension is a color for painting. Actions with high enough water or heat levels wash or dry a held widget, respectively; actions with paint colors that are close enough to either the shelf or box color result in painting the held object that color; otherwise, the action results in a pick, a place, or no effect, depending on whether an object is currently held, the target gripper state is near enough to either “open” or “closed,” and whether the current end effector rotation matches the requirements of the desired placement (box placements require top grasps; shelf placements require side grasps). Picking a box lid has the effect of opening it. The **behavior prior** randomly picks, washes, dries, paints, or places objects. The **predicates** are: ONTABLE, HOLDING, HOLDINGSIDE, HOLDINGTOP, INSHELF, INBOX, ISDIRTY, ISCLEAN, ISDRY, ISWET, ISBLANK, ISSHELFCOLOR, ISBOXCOLOR, all parameterized by a single ?WIDGET,

and `GRIPPEROPEN(?`ROBOT`)`. Across all tasks, there is only one robot, box, lid, and shelf, and the goal is to paint each widget a certain color (each box or shelf color) and place it in the corresponding receptacle. **Training tasks** feature 2 or 3 widgets, and have horizon $H = 18$. **Easy test tasks** feature 1 widget, and have horizon $H = 6$. **Hard test tasks** feature 10 widgets, and have horizon $H = 60$.

A.3 Extended Method Details

Here, we provide additional details about the methods.

The NSRT action samplers and low-level effect models are always fully connected neural networks with hidden layer sizes [32, 32]. During evaluation only, we clip samples from the action samplers to be at most 1 standard deviation from the mean, for improved stability. The applicability classifier is also a fully connected neural network with hidden layer sizes [32, 32]. We subsample negative data to ensure that it is balanced, in a 1:1 ratio, with the positive data. Neural networks are trained using the Adam optimizer [Kingma and Ba, 2014] for 35K (action samplers), 10K (low-level effect models), or 50K (applicability classifier) epochs, always with a learning rate of 1e-3.

For implementing the h_{add} heuristic, we use the Pyperplan [Alkhazraji et al., 2020] software package.

All GNNs (both the collision predictor, and the action-value function of B4) are standard encode-process-decode architectures [Battaglia et al., 2018], where node and edge modules are fully connected neural networks with one hidden layer of dimension 16, ReLU activations, and layer normalization. Message passing is performed for $K = 3$ iterations. Training uses the Adam optimizer [Kingma and Ba, 2014] for 500 epochs with learning rate 1e-3 and batch size 128. For the action-value function, we train by running 5 iterations of fitted Q-iteration, and during evaluation, we sample 100 candidate actions from the behavior prior π_0 at each step, choosing the action with the best predicted value to execute in the environment.

Methods that use shooting (B2 and B7) try up to 1000 iterations, or until the timeout (3 seconds for every method across all experiments) is reached. Methods that perform rejection sampling from the behavior prior (B6 and B7) with the learned applicability classifiers try up to 30 times before giving up and returning a random action from the behavior prior.

Figure 3 shows that B4 (the action-value function learning baseline) performs very poorly. In preliminary experiments, we had verified that it works in much easier test task instances than were used for any of our main results in Figure 3. The main finding from those preliminary experiments was that action-value function learning requires a lot more data than we are working with in this paper; B4 began to perform at the level of our approach given about 2000 training episodes, on those very easy test task instances (whereas our main results are only conducted up to 500 training episodes). This finding is consistent with the general principle that model-free learning strategies are known to be data-hungry [Moerland et al., 2020].

A.4 Ablation Standard Deviation Results

Table 2 reports the standard deviations for the ablation experiments, accompanying the means shown in Table 1. They were omitted from Table 1 due to space reasons. See Section 7 for details.

Methods	PickPlace1D		Kitchen		Blocks		Painting	
	Easy	Hard	Easy	Hard	Easy	Hard	Easy	Hard
Bilevel planning with NSRTs (Ours)	2.826	15.492	0.599	2.736	1.414	3.935	0.696	8.731
Bilevel planning with prior (B6)	3.140	8.425	9.778	10.295	5.510	10.735	15.882	0.331
Forward shooting with prior (B7)	4.106	0.000	0.000	1.323	4.807	2.736	3.276	0.000

Table 2: This table is a companion to Table 1 in the main text, showing the numerical standard deviations of the means. See Table 1 caption for details.